Geophysical Research Letters

RESEARCH LETTER
10.1029/2020GL090675

Key Points:

- A novel, satellite-based method was developed to retrieve profiles of convective vertical velocity (w_c) and convective mass flux (M_c)
- Comparisons with collocated ground-based radar wind profiler observations show broad agreements
- A *k*-means cluster analysis shows that convective vertical velocity is distinctly different between tropical land and oceanic convection

Correspondence to:
Z. J. Luo,
zluo@ccny.cuny.edu

Citation:
Jeyaratnam, J., Luo, Z. J., Giangrande, S. E., Wang, D., & Masunaga, H. (2021). A satellite-based estimate of convective vertical velocity and convective mass flux: Global survey and comparison with radar wind profiler observations. *Geophysical Research Letters*, *48*, e2020GL090675. https://doi.org/10.1029/2020GL090675

Received 4 SEP 2020
Accepted 24 NOV 2020

© 2020. American Geophysical Union. All Rights Reserved.

A Satellite-Based Estimate of Convective Vertical Velocity and Convective Mass Flux: Global Survey and Comparison With Radar Wind Profiler Observations

Jeyavinoth Jeyaratnam[1], Zhengzhao Johnny Luo[2], Scott E. Giangrande[3], Dié Wang[3], and Hirohiko Masunaga[4]

[1]The Graduate Center, Earth and Environmental Sciences Program, City University of New York, New York, NY, USA, [2]Department of Earth and Atmospheric Sciences, City University of New York, City College, New York, NY, USA, [3]Department of Environmental and Climate Sciences, Brookhaven National Laboratory, Upton, NY, USA, [4]Institute for Space-Earth Environmental Research, Nagoya University, Nagoya, Japan

Abstract Convective vertical velocity (w_c) and convective mass flux (M_c) lie at the heart of global climate model cumulus parameterizations, but few observations of these critical parameters are available. This paper develops and evaluates a novel, satellite-based method for estimating profiles of w_c and M_c. Comparisons with collocated ground-based radar wind profiler (RWP) observations show that satellite-estimated median w_c is slightly greater than the RWP estimates, but they show solid agreement when compared at the 95th percentiles (intense updrafts). RWP-derived and satellite-estimated M_c are broadly comparable in the lower and middle troposphere, with some differences in the upper troposphere due to differences in convective core sampling. A *k*-means cluster analysis of multiple years of w_c data shows that convective characteristics are distinctly different among extratropical convection, tropical land convection, and tropical oceanic convection. Tropical land convection is significantly more intense and more variable than the oceanic counterpart.

Plain Language Summary Properly representing and parameterizing cumulus convection has long been a central task of the global climate models (GCMs), as GCM simulations are highly sensitive to the assumptions made in the cumulus parameterization schemes, resulting in large uncertainties in predicting the future climate change. At the heart of many of today's GCM convection parameterizations are convective vertical velocity (w_c) and mass flux (M_c). Yet, few global observations of these critical parameters are available at this time globally. To improve this situation, the authors developed a novel, satellite-based method for estimating profiles of w_c and M_c. We first evaluate the satellite estimates against collocated ground-based radar wind profiler (RWP) retrievals. RWP-derived and satellite-estimated w_c and M_c are found to be broadly comparable, and their agreement improves when differences in sampling and definitions of convective clouds are considered. A *k*-means cluster analysis of multiple years of satellite-estimated w_c data is performed to identify salient patterns related to the structure and global distributions of convective vertical velocity. Results show that convective characteristics are distinctly different among extratropical convection, tropical land convection, and tropical oceanic convection. Our ongoing work seeks to use this newly developed w_c and M_c data set to evaluate GCM cumulus parameterizations.

1. Introduction

Convection is fundamental to atmospheric energetics and general circulation. While the ultimate energy source for Earth's atmosphere comes from the Sun, most of the solar insolation is directly deposited at the surface. Convection redistributes the energy by transporting it from the surface upward into the atmosphere, balancing atmospheric cooling in the infrared, and driving large-scale circulation (e.g., Hartmann, 2016). In doing so, convection also moves momentum, moisture, and chemically important trace constituents from the planetary boundary layer to the free troposphere. Deep convection can even communicate these influences all the way to the upper troposphere and lower stratosphere (e.g., Fueglistaler et al., 2009). For these reasons, properly representing convection and convective transport has always been a central task of the global climate models (GCMs) (e.g., Arakawa, 2004).

Because convective core occurs on the scale of O(1–10 km) which is smaller than the grid box of current GCMs (O[100 km]), cumulus convection cannot be explicitly represented and has to be parameterized as a function of grid-scale variables. GCM simulations are highly sensitive to the assumptions made in the parameterizations, resulting in large uncertainties in our ability to predict the future climate change (e.g., Sanderson et al., 2008). A large number of current GCM cumulus parameterization schemes are based on the concept of convective mass flux (defined as the product of air density, convective cloud coverage, and vertical velocity), and tied to the model's large-scale variables via a closure scheme (see Arakawa, 2004 for a review). Improved assessment of the fidelity for cumulus parameterizations requires new ways to observe convective mass flux globally.

The most challenging part for obtaining convective mass flux is estimating the vertical air motions inside deep convective clouds (DCCs). Historically, the most direct observational approach was to fly instrumented aircraft into DCCs to measure the vertical air velocity and other updraft/downdraft core properties *in situ*. Over the past 70 years, numerous storm penetration flights have enabled important firsthand knowledge of the inner workings of DCCs (e.g., Byers & Braham, 1948; LeMone & Zipser, 1980a, 1980b; Lucas et al., 1994). However, operational costs and safety concerns place severe constraints on such flights, limiting the available data sets while significantly under-sampling the strongest cloud drafts. As an alternative, high-altitude aircraft may fly above convective storms and use a nadir-viewing Doppler radar to retrieve convective air motions. For example, a 10-year summary of overflight measurements from numerous field campaigns have been compiled and analyzed by Heymsfield et al. (2010) to characterize DCCs from various environments in the tropics and subtropics. In a similar fashion, ground-based (multi-) Doppler radars and wind profilers have been exploited using various methodologies to estimate convective vertical velocities remotely (Giangrande et al., 2013, 2016; Kumar et al., 2015; May & Rajopadhyaya, 1999; North et al., 2017; D. Wang et al., 2019, 2020; Williams, 2012). These ground-based retrievals, in particular those from vertically pointing radar wind profilers (RWPs), afford continuous and long-term measurements in deeper and midlatitude convective clouds where prior *in situ* or overpass aircraft estimates are limited.

Although these above-mentioned observational studies provide valuable insights into convective vertical velocity and mass flux, available observations of the convective cloud kinematic properties are limited in space and time, especially over the tropics and open oceans, making it difficult to generalize such findings globally for developing or evaluating GCM cumulus parameterizations (Donner et al., 2001, 2016). Observations from satellites offers a potential solution to the problem. However, no current satellite is designed for estimating the vertical air motions inside convective clouds. Although plans for deploying space-borne Doppler cloud radars have been undertaken for the near future (e.g., EarthCARE mission; Illingworth et al., 2015), severe attenuation of W-band (94-GHz) or similar cloud radar through heavy precipitation makes it challenging to retrieve vertical velocity profiles inside convective cores (Z. J. Luo et al., 2014). To fill the vacuum, a novel, satellite-based method has been proposed in a recent study by Masunaga and Luo (2016; hereafter ML16). Unlike previous radar-based methods that focus on measurements of each individual cloud, ML16 brings together multiple information including the observed state of convective cloud, as well as constraints such as the ambient sounding and underlying dynamic and thermodynamic principles by which convective cloud is bound to abide (i.e., a plume model), and then combines them in a Bayesian manner to estimate convective vertical velocity and mass flux.

This current study builds upon ML16 with the following two motivations: 1) Evaluate satellite estimates of convective vertical velocity and mass flux with collocated ground-based RWP observations made by Department of Energy (DOE) Atmospheric Radiation Measurement (ARM) program (Section 3). Focus is placed on the updrafts in convective clouds. 2) Extend ML16 study (that emphasized equatorial oceanic region) over the entire globe to identify major global patterns of convective cloud kinematics (Section 4). Section 5 summarizes the study and discusses its significance and future applications.

2. Data and Methodology

2.1. Data Description

Satellite data used for this study come from the A-Train constellation (Stephens et al., 2002), mainly CloudSat Cloud Profiling Radar (CPR; Stephens et al., 2008), Cloud-Aerosol Lidar and Infrared Pathfinder Satellite

Observation (CALIPSO) Cloud-Aerosol Lidar with Orthogonal Polarization (CALIOP; Winker et al., 2010), and Moderate Resolution Imaging Spectroradiometer (MODIS). The variables relevant to the ML16 method include 1) CPR and CALIOP cloud-top height, and 2) CPR reflectivity profiles, both obtained from CloudSat 2B-GEOPROF-LIDAR product (Mace & Zhang, 2014), and 3) MODIS infrared brightness temperature, obtained from standard MODIS radiance data (Platnick et al., 2003). The CloudSat CPR footprint size is 2.3 km along track and 1.4 km cross track, and the effective vertical resolution is 480 m, oversampled at 240 m. CALIOP data have higher horizontal and vertical resolutions, but they are anchored on CPR profiles in the 2B-GEOPROF-LIDAR data such that the effective resolutions are reduced to match those of CPR. MODIS infrared brightness temperatures have horizontal resolution of 1 km. ML16 also used sounding data from satellite sounders. In this study, we use collocated European Centre for Medium-Range Weather Forecast (ECMWF) operational analyses that were obtained from the ECMWF-AUX product of CloudSat and have the horizontal resolution of 0.5°.

Ground-based data are obtained from measurements collected by the DOE ARM (Mather & Voyles, 2013) Mobile Facility (AMF) at Manacapuru, Brazil (MAO) during the "Observations and Modeling of the Green Ocean Amazon 2014–2015" (GoAmazon 2014/5, e.g., Martin et al., 2017) field campaign. The primary observations used are convective cloud vertical velocity and mass flux derived from vertically pointing RWP measurements operated at ultrahigh frequencies (1,290 MHz at MAO). The RWPs are not attenuated in rain owing to their long wavelength, and calibrated using collocated disdrometer observations (e.g., D. Wang et al., 2018). These measurements were made in time-height space at ~10-s temporal and 200-m gate resolutions using operational precipitation modes employed by ARM that are not susceptible to Bragg echo contamination in deep convective contexts (e.g., Tridon et al., 2013). Estimates of vertical velocity at DCCs and periphery regions follow the retrieval methods described in Giangrande et al. (2013; 2016) and D. Wang et al. (2020).

2.2. A Brief Description of ML16 Method

ML16 developed a hybrid method to estimate convective vertical velocity (w_c) and convective mass flux (M_c). Input information comes from three main sources: ambient sounding, plume model, and satellite cloud observations. These inputs are combined in a Bayesian manner to produce estimates of w_c and M_c. In Figure 1, we use a flowchart to schematically illustrate this procedure. First, CloudSat CPR reflectivity profiles are used to identify convective cores following early studies by Z. Luo et al. (2008, 2009) and Z. J. Luo et al. (2010), as illustrated in Figures 1a and 1c. A convective core is defined as consecutive radar profiles that contain continuous radar echoes extending from the planetary boundary layer to cloud top, with 10 dBZ echo-top height being within 2 km of cloud top. The cloud-top buoyancy factor, represented by $\left(T_c - T_a\right) / T_a$ is estimated for each convective core following Z. J. Luo et al. (2010), where T_c is cloud-top temperature and T_a is the ambient temperature of the same level. T_c is estimated from MODIS IR brightness temperature after accounting for parallax shift of MODIS relative to CloudSat and CALIPSO (C. Wang et al., 2011) and nonblackbody effect in the infrared (C. Wang et al., 2014). T_a is obtained from the collocated ECMWF analyses.

CloudSat observations along track are divided into segments of O(100 km); each is comparable to a GCM grid box. Then, ambient temperature and moisture sounding at each segment drives the convective plume model, which generates a range of in-cloud buoyancy and vertical velocity profiles. The main unknown parameter (to be constrained by observations) in this process is the turbulent entrainment rate, which is assumed to vary by a wide range from 0 to 0.4 km^{-1}, following ML16. This step is schematically shown in Figures 1b and 1d. Next, the observed cloud-top buoyancy of each convective core is used to weigh the plume model simulations via a Bayesian approach to arrive at a final estimate of buoyancy and w_c profiles, as illustrated in Figures 1e and 1f.

Finally, convective mass flux M_c is calculated as $M_c = \sigma \rho w_c$, where σ is the coverage of convective clouds and ρ is air density. Convective coverage σ is estimated from CloudSat CPR profiles and is determined by counting the fractional coverage of convective cores within each segment as illustrated in Figure 1g. Air density ρ is obtained from the collocated ECMWF analyses. For a complete description of the ML16 method, including the plume model and Bayesian formula, see Section 3 of ML16.

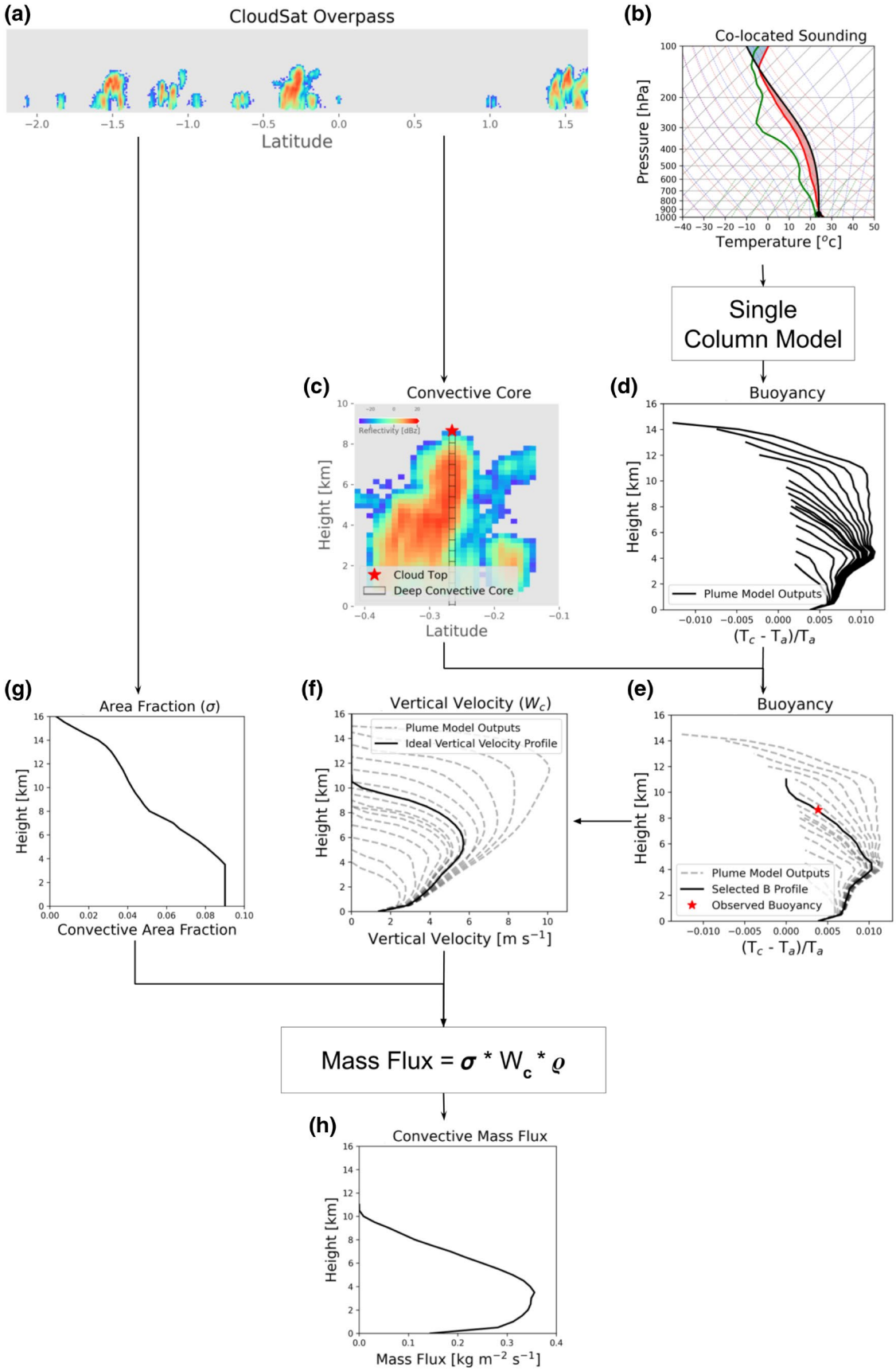
(a)
CloudSat Overpass
Latitude
(b)
Co-located Sounding
Pressure [hPa]
Temperature [°c]
Single Column Model
(c)
Convective Core
Reflectivity [dBZ]
Height [km]
Cloud Top
Deep Convective Core
Latitude
(d)
Buoyancy
Height [km]
Plume Model Outputs
(Tc - Ta)/Ta
(g)
Area Fraction (σ)
Height [km]
Convective Area Fraction
(f)
Vertical Velocity (Wc)
Plume Model Outputs
Ideal Vertical Velocity Profile
Height [km]
Vertical Velocity [m s−1]
(e)
Buoyancy
Height [km]
Plume Model Outputs
Selected B Profile
Observed Buoyancy
(Tc - Ta)/Ta
Mass Flux = σ * Wc * ϱ
(h)
Convective Mass Flux
Height [km]
Mass Flux [kg m−2 s−1]

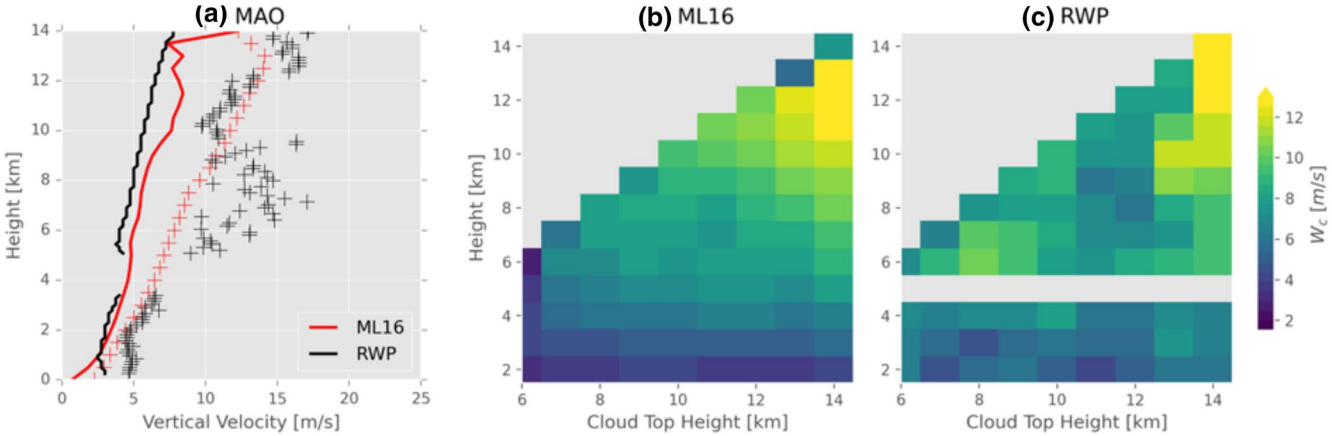

Figure 2. (a) Convective vertical velocity profiles from ground-based RWP observations (black) and ML16 estimates (red). Solid lines represent the median profiles, and crosses represent the 95th percentiles (i.e., intense updrafts). (b) ML16 retrieved convective vertical velocity profiles sorted by convective depth. Only the 95th percentiles are shown. (c) Same as (b), except for RWP estimates.

The ML16 method only considers convective updrafts. Downdrafts are not easily identified from CloudSat radar reflectivity profiles. The contribution of downdraft mass flux can be indirectly inferred from the difference between total mass flux and convective updraft mass flux, as demonstrated in ML16. However, determination of total mass flux requires additional measurements that are not available globally (e.g., wind fields from QuickSCAT, available only over ocean; see ML16). Therefore, we confine this study to updraft properties and leave the consideration of downdrafts to a future study. For a fair comparison, only updraft properties (and their fractional coverage) estimated by the RWP observations are used.

3. Comparison Between Satellite Estimates and Radar Wind Profiler Observations

RWP and satellite estimates use different sampling strategies and retrieval methods. Therefore, a meaningful comparison is only possible in a statistical sense. Similar to previous observational studies that attempt to extract convective mass flux profiles over GCM-scale grids (e.g., Kumar et al., 2015), we use 3-hourly averages, aggregated over long-term RWP observations (translates to a spatial domain of about 60-km, assuming an average propagation speed of 5 m s^{-1}). This procedure is intended to align these column observations with the proposed satellite estimates collected in a 0.5° × 0.5° box around the ARM MAO site. Comparisons are performed for the entire 2-year GoAmazon2014/5 field campaign.

Figure 2a shows the summary comparisons of w_c profiles in terms of the updraft median and 95th percentile properties. Both RWP observations and satellite estimates show that w_c generally increases with height, a feature that is commonly observed in DCCs (Giangrande et al., 2016; Heymsfield et al., 2010; Kumar et al., 2015; D. Wang et al., 2019, 2020). This is in line with the expectation that buoyancy acceleration within convective updraft is usually positive until air parcel overshoots which usually occurs at high altitudes near cloud top (Z. J. Luo et al., 2010; Takahashi & Luo, 2012; Takahashi et al., 2017). Note, median w_c values are slightly larger for satellite estimates than RWP values. This difference may be attributed to different sampling strategies as to defining "core" regions: the RWP vertical velocity profiles include contributions from intense convective updraft cores and the periphery DCC regions, provided that the measured vertical velocity exceeds 1.5 ms^{-1} (Giangrande et al., 2016; D. Wang et al., 2020). However, the ML16 method is designed to characterize the vertical velocity of only the well-defined and active updrafts captured by CloudSat CPR. To account for some of these differences, we also estimate the 95th percentile velocities from both platforms

Figure 1. Schematic flowchart illustrating the procedure of estimating convective vertical velocity (w_c) and convective mass flux (M_c), as developed in Masunaga and Luo (2016) or ML16.

(crosses in Figure 2a) that focus only on the more intense updrafts/core properties. Now, the systematic bias seen in the median w_c is no longer evident. A better agreement is seen in comparison of the 95th percentiles, especially in the upper troposphere. A local spike is seen in the RWP 95th percentile vertical velocity profile at the altitudes of 6–8 km. One physical interpretation is that this spike could be attributed to additional buoyancy added through latent heating release from fusion and freezing above the melting level (Zipser, 2003) that is not precisely reproduced by the simplified microphysics built in the plume model. However, this spike may also reflect a practical consequence of conditional sampling bias, wherein the RWP retrievals/extremes for DCC "hits" are less frequently captured (and therefore prone to variability) at these altitudes.

To gain further insight into convective cloud structure, we sort vertical velocity profiles by radar echo-top height, which serves as a proxy for convective depth (Figures 2b and 2c), following D. Wang et al. (2019). This sorting better differentiates the properties for the different modes of convection (e.g., deep convection, cumulus congestus, and shallow convection, Johnson et al., 1999). Since RWP and satellite estimates are initially comparable in their capability to gauge intense updrafts (see Figure 2a), our focus is on the 95th percentile properties. Not surprisingly, Figures 2b and 2c suggest that DCCs have larger vertical velocity than shallower convection, while vertical velocity estimates tend to peak at the upper parts of the clouds. Both of these characteristics are consistent with our understanding of buoyancy distribution within convective updrafts (ML16). Here, Figures 2b and 2c show that these convective vertical velocity tendencies compare favorably between the ground-based RWP observations and proposed satellite estimates, although the absolute values are slightly different. The RWP estimates also appear more sensitive to the frequent cumulus congestus mode found in the Amazon.

In Figure 3a, we plot a comparison for retrievals of domain-mean convective mass flux profile, with the shaded region representing the range of retrieval variation as a result of varying the grid box for collecting satellite data around the ARM site from 0.25° to 0.75° (solid curve is for 0.5° box). Figure 3a suggests that the RWP and satellite-estimated convective mass fluxes are broadly comparable in the lower and middle troposphere (<6 km), but show some differences in the upper troposphere. Unlike vertical velocity that increases with height, convective mass flux peaks in the lower to middle troposphere because it is largely modulated by fractional coverage of convective clouds ($M_c = \sigma\rho w_c$). This change in peak is associated with convective cloud fraction (σ) that tends to decrease with height due to the more abundant presence (fractional) of shallow convection and cumulus congestus. To further investigate the roles played by different constituents of convective mass flux, we examine the variations of w_c, σ, and M_c between the traditional Amazonian wet (December to March) and dry (June to September) regimes, following Giangrande et al. (2016) and D. Wang et al. (2019). Figures 3b–3d together suggest that convective vertical velocity properties are similar between the wet and dry season (slightly larger for the dry season in the upper troposphere), but convective mass flux is about twice as large during the wet season, because variation of convective mass flux is primarily controlled by that of convective cloud coverage, with the mean vertical velocity playing a secondary role. Similar findings were also reported in previous studies by Kumar et al. (2015), Giangrande et al. (2016), and Masunaga and Luo (2016). Most of the discrepancy between satellite and ground-based estimate of convective (updraft) mass flux in Figure 3a can be attributed to the difference in convective cloud coverage due to different sampling interpretations. Specifically, the proposed satellite retrievals only consider a stringent (thus narrow) convective core definition, whereas the RWP mass flux profile estimates allow a wider convective area having vertical velocity > 1.5 ms^{-1}. This difference is especially important in the upper troposphere, where some periphery core to anvil regions are included in RWP area fractions. This explains why most of the satellite and RWP estimate differences are located in the upper troposphere. These comparison results point to the importance for properly accounting for the fractional coverage of convective clouds and platform sensitivity therein, as well as updraft fraction as a function of height when retrieving mass flux profiles at GCM grid scale for model evaluation.

4. Global Patterns of Convective Vertical Velocity

By applying the proposed satellite retrievals to the larger global data set, one could investigate general patterns related to the structures and distributions of convective vertical velocity and mass flux. Here, we perform the standard *k*-means cluster analysis (e.g., Anderberg, 1973) on 2 years of w_c profile data globally. As

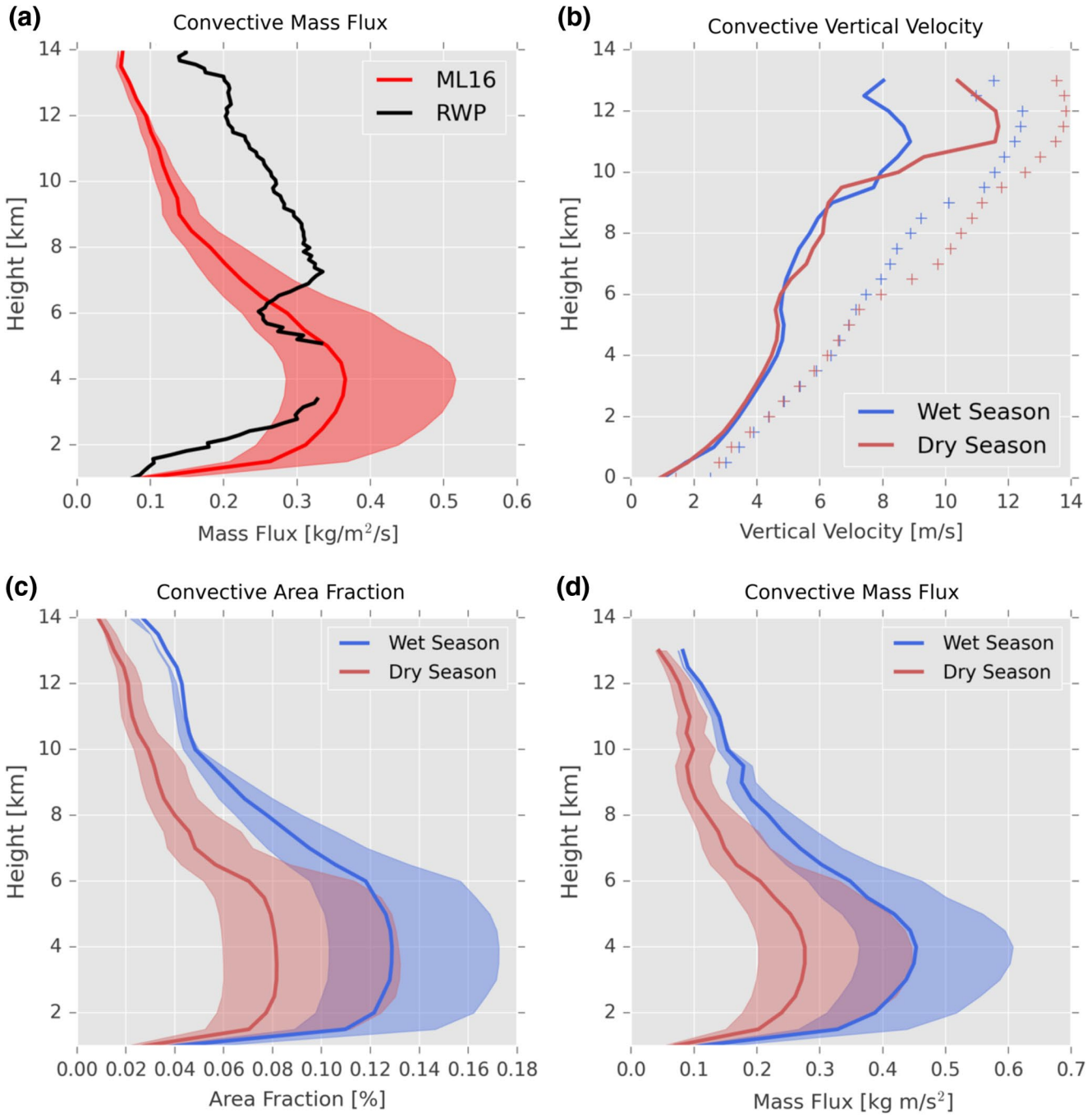

Figure 3. (a) Mean convective mass flux ($M_c = \sigma\rho w_c$) profiles estimated from the RWP observations (black) and satellite estimates (red). The shaded region represents the range of retrieval variation as a result of varying the grid box for collecting satellite data around the ARM site. See texts for details. (b) Satellite-derived convective vertical velocity (w_c) for the Amazonian wet (blue) and dry (red) regimes. Solid lines represent the mean profiles, and crosses represent the 95th percentiles. (c) Satellite-derived convective area fraction (σ) for the Amazonian wet (blue) and dry (red) regimes. The shaded region represents the same variation associated with grid box size as in (a). (d) Same as (c), but for convective mass flux (M_c).

described in Section 3, satellite data are collected and analyzed for 0.5° × 0.5° grid boxes around the ARM MAO site providing measurements at a spatial scale that could be evaluated against RWP concepts, but also aligning with basic GCM-driven evaluation considerations. Following this, we divide the whole globe within the latitude range of 45°S-45°N into 0.5° × 0.5° grids (higher latitudes are excluded in this study because convection is less frequent there), and in each grid, the retrieved convective vertical velocity profiles

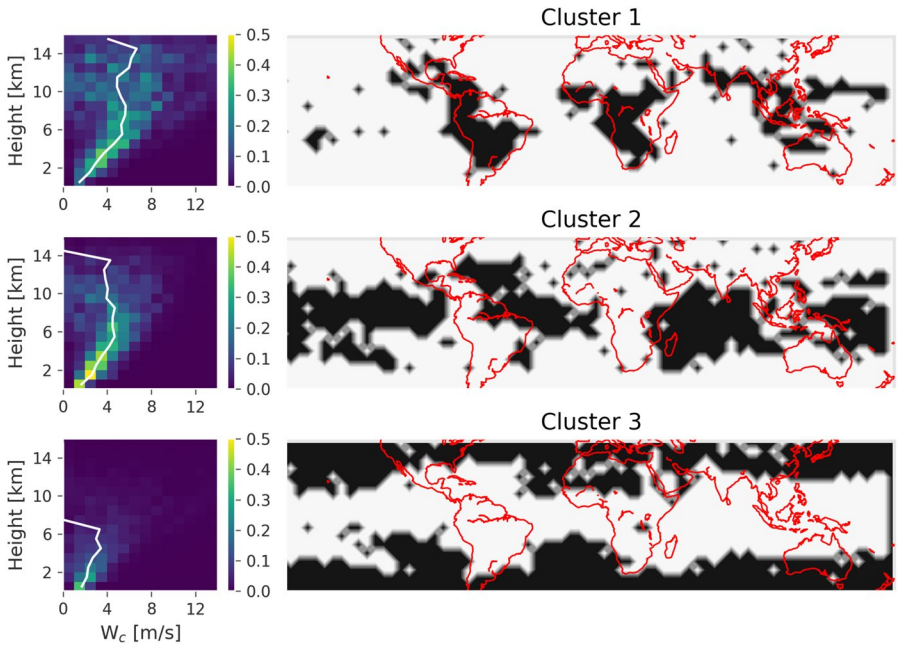

Figure 4. Centroids of the three clusters in terms of height-w_c histograms. The contour value refers to the frequency of occurrence for each height level and the white line shows the mean w_c values (left). Geographical distribution of these clusters. Black color at each 0.5° × 0.5° grid means the grid is associated with the corresponding cluster (right).

are compiled in a height-w_c histogram to summarize the characteristics of their vertical structures, similar to the contoured frequency by altitude diagram by Yuter and Houze (1995). The k-mean cluster analysis is performed on these height-w_c histograms.

Three clusters emerge from the k-means analysis (sensitivity tests show that $k = 3$ is the optimal choice). Figure 4 shows the centroids of the clusters in terms of height-w_c histograms and the corresponding geographical distributions (note that each 0.5° × 0.5° grid is associated with only one of the three clusters). The three clusters are distinctly separated geographically: the first cluster corresponds to convection over tropical land and the second to convection over tropical ocean. The third cluster is mostly associated with convection in the extra-tropics, some of which may be embedded in extratropical cyclones (Jeyaratnam et al., 2020). The height-w_c histograms clearly show the associated differences in vertical structures: 1) Convection in the tropics is generally deeper than the extratropical convection, due to higher tropopause in the tropics. 2) Tropical land convection tends to be more intense and more variable than the oceanic counterpart. For example, the height-w_c histograms in Figure 4 shows that in the upper troposphere, the mean value for w_c is about 50% larger over land (Cluster 1) than over ocean (Cluster 2), and the standard deviation is more than 4 times as large over land (Cluster 1) as over ocean (Cluster 2).

These regional differences in convective characters are not entirely unexpected, as similar characteristics have been documented in a number of previous studies. For example, tropical land convection containing stronger updrafts than the oceanic counterpart has been observed by both cloud-penetrating aircraft (Lucas et al., 1994) and airborne Doppler radars (Heymsfield et al., 2010). Similarly, TRMM and CloudSat radar echo-top heights also indirectly point to this potential land-ocean contrast (e.g., Liu et al., 2007; Takahashi & Luo, 2012; Takahashi et al., 2017). Nevertheless, it is remarkable to see these bulk differences show up unambiguously and globally in extended satellite estimates of convective vertical velocity. It should be noted that no artificial or external rule is imposed on our analysis to trigger the land-ocean and tropics-midlatitude separations. They are entirely the result of an untrained, statistical analysis. Moreover, running a similar k-means cluster analysis on the ambient sounding data does not produce such a clear land-ocean separation (not shown). These results clearly point to the fundamental nature of these regional differences in convective cloud characters. Furthermore, our analyses suggest that a Bayesian combination of satellite observations, the ambient sounding, and a plume model—a key feature of our satellite retrieval

method—add values to the input data sources toward a more complete characterization of the structure and distribution of convective vertical velocity.

5. Summary and Discussions

Convective vertical velocity (w_c) and mass flux (M_c) lie at the heart of GCM cumulus parameterizations, yet few observations of these critical parameters are available at this time. To improve this situation in a manner amenable to global scales, ML16 developed a novel method using space-borne measurements, aided by a plume model driven by the ambient sounding, to estimate profiles of w_c and M_c. This current study is a follow on to ML16, with the primary purposes being: 1) to compare ML16 satellite estimates of convective w_c and M_c with ground-based RWP observations made by the DOE ARM program and 2) to apply ML16 method to global scales to identify salient patterns related to the structure and global distributions of convective vertical velocity. The main findings are as follows:

1. Satellite and RWP estimates show the general trend that convective vertical velocity increases with height. Satellite-estimated vertical velocity is slightly stronger than that retrieved by RWPs when comparing median profile behaviors, with this difference attributed to differences in the definitions for allowable convective regions. When compared by vertical velocity properties at the 95th percentile levels, such systematic difference is no longer as evident between satellite and RWP estimates, and there is generally solid agreement between these estimates.
2. RWP-derived and satellite-estimated convective mass fluxes are broadly comparable in the lower and middle troposphere, but show some differences in the upper troposphere. Analysis of different constituents of convective mass flux shows that M_c is primarily controlled by fractional coverage of convective clouds, with the mean vertical velocity playing a secondary role, confirming findings from several recent studies.
3. *K*-means cluster analysis of multiple years of global (45°S-45°N) convective vertical velocity data shows that convective characteristics are distinctly different among extratropical convection, tropical land convection, and tropical oceanic convection. Generally, tropical convection is deeper, while tropical convection over land is more intense and variable than the oceanic counterpart.

Developing global observations of convective vertical velocity and mass flux is critical to understanding the complicated nature of convective dynamics and to evaluating their representations in GCMs. ML16 and this current study represent a first step toward this goal. Comparisons with ground-based observations are mostly positive, although there are discrepancies due to differences in observational methods and sampling strategy. A simple clustering analysis leads to valuable insights into fundamental differences in convective characters in different environments. Our ongoing work seeks to use the newly developed data to evaluate GCM cumulus parameterizations.

Data Availability Statement

CloudSat and DOE ARM data are publicly available for all researchers and can be obtained at http://www.cloudsat.cira.colostate.edu/ and https://arm.gov/, respectively.

Acknowledgments
This work was mainly supported by the following NASA grants awarded to CUNY under 80NSSC17K0197, 80NSSC18K1600, and 80NSSC20K0089. S. E. Giangrande and D. Wang are supported by U.S. DOE contract DE-SC0012704. The publisher by accepting the paper for publication acknowledges that the U.S. Government retains a nonexclusive, paid-up, irrevocable, worldwide license to publish or reproduce the published form of this paper or allow others to do so, for U.S. Government purposes. The authors would like to acknowledge fruitful discussions with Drs. W. B. Rossow, A. D. Del Genio, M. P. Jensen, and G. Elsaesser.

References

Anderberg, M. R. (1973). *Cluster analysis for applications*. New York, NY: Elsevier. pp. 359.
Arakawa, A. (2004). The cumulus parameterization problem: Past, present, and future. *Journal of Climate*, *17*, 2493–2525.
Byers, H. R., & Braham, R. R. Jr (1948). Thunderstorm structure and circulation. *Journal of Meteorology*, *5*, 71–86.
Donner, L. J., O'Brien, T. A., Rieger, D., Vogel, B., & Cooke, W. F., (2016) Are atmospheric updrafts a key to unlocking climate forcing and sensitivity? *Atmospheric Chemistry and Physics*, *16*, 12983–12992. https://doi.org/10.5194/acp-16-12983-2016
Donner, L. J., Seman, C. J., Hemler, R. S., & Fan, S. (2001). A cumulus parameterization including mass fluxes, convective vertical velocities, and mesoscale effects: Thermodynamic and hydrological aspects in a general circulation model. *Journal of Climate*, *14*, 3444–3463. https://doi.org/10.1175/1520-0442(2001)014<3444:ACPIMF<2.0.CO
Fueglistaler, S., Dessler, A. E., Dunkerton, T. J., Folkins, I., Fu, Q., & Mote, P. W. (2009). Tropical tropopause layer. *Review of Geophysics*, *47*, RG1004. https://doi.org/10.1029/2008RG000267

Giangrande, S. E., Collis, S., Straka, J., Protat, A., Williams, C., & Krueger, S. (2013). A summary of convective-core vertical velocity properties using ARM UHF wind profiler in Oklahoma. *Journal of Applied Meteorology and Climatology*, *52*, 2278–2295.

Giangrande, S. E., Toto, T., Jensen, M. P., Barrtholomew, M. J., Feng, Z., & Protatett, A. (2016). Convective cloud vertical velocity and mass-flux characteristics from radar wind profiler observations during GoAmazon2014/5. *Journal of Geophysical Research: Atmosphere*, *121*(12), 891–913. https://doi.org/10.1002/2016JD025303

Hartmann, D. L., (2016). *Global physical climatology*. Elsevier Inc. 485 pp.

Heymsfield, G. M., Tian, L., Heymsfield, A. J., Li, L., & Guimond, S. (2010). Characteristics of deep tropical and subtropical convection from nadir-viewing high-altitude airborne Doppler radar. *Journal of the Atmospheric Sciences*, *67*, 285–308.

Illingworth, A. J., Barker, H. W., Beljaars, A., Ceccaldi, M., Chepfer, H., & Clerbaux, N. et al. (2015). The EarthCARE Satellite: The next step forward in global measurements of clouds, aerosols, precipitation, and radiation. *Bulletin of the American Meteorological Society*, *96*(8), 1311–1332.

Jeyaratnam, J., Booth, J. F., Naud, C. M., Luo, Z. J., & Homeyer, C. R. (2020). Upright convection in extratropical cyclones: A survey using ground-based radar data over the United States. *Geophysical Research Letters*, *47*, e2019GL086620. https://doi.org/10.1029/2019GL086620

Johnson, R. H., Rickenbach, T. M., Rutledge, S. A., Ciesielski, P. E., & Schubert, W. H. (1999). Trimodal characteristics of tropical convection. *Journal of Climate*, *12*, 2397–2418.

Kumar, V. V., Jakob, C., Protat, A., Williams, C. R., & May, P. T. (2015). Mass-flux characteristics of tropical cumulus clouds from wind profiler observations at Darwin, Australia. *Journal of the Atmospheric Sciences*, *72*, 1837–1855. https://doi.org/10.1175/JAS-D-14-0259.1

LeMone, M. A., & Zipser, E. J. (1980a). Cumulonimbus vertical velocity events in GATE. Part I: Diameter, intensity, and mass flux. *Journal of the Atmospheric Sciences*, *37*, 2444–2457.

LeMone, M. A., & Zipser, E. J. (1980b). Cumulonimbus vertical velocity events in GATE. Part II: Synthesis and model core structure. *Journal of the Atmospheric Sciences*, *37*, 2458–2469.

Liu, C., Zipser, E. J., & Nesbitt, S. W. (2007). Global distribution of tropical deep convection: Different perspectives from TRMM infrared and radar data. *Journal of Climate*, *29*(3), 489–503.

Lucas, C., Zipser, E. J., & LeMone, M. A. (1994). Vertical velocity in oceanic convection off tropical Australia. *Journal of the Atmospheric Sciences*, *51*, 3183–3193.

Luo, Z. J., Jeyaratnam, J., Iwasaki, S., Takahashi, H., & Anderson, R. (2014). Convective vertical velocity and cloud internal vertical structure: An A-Train perspective. *Geophysical Research Letters*, *41*. https://doi.org/10.1002/2013GL058922

Luo, Z., Liu, G. Y., & Stephens, G. L. (2008). CloudSat adding new insight into tropical penetrating convection. *Geophysical Research Letters*, *35*, L19819. https://doi.org/10.1029/2008GL035330

Luo, Z. J., Liu, G. Y., & Stephens, G. L. (2010). Use of A-Train data to estimate convective buoyancy and entrainment rate. *Geophysical Research Letters*, *37*, L09804. https://doi.org/10.1029/2010GL042904

Luo, Z., Liu, G. Y., Stephens, G. L., & Johnson, R. H. (2009). Terminal versus transient cumulus congestus: A CloudSat perspective. *Geophysical Research Letters*, *36*, L05808. https://doi.org/10.1029/2008GL036927

Mace, G. G., & Zhang, Q. (2014). The CloudSat radar-lidar geometrical profile product (RLL-GeoProf): Updates, improvements, and selected results. *Journal of Geophysical Research: Atmospheres*, *119*, 9441–9462. https://doi.org/10.1002/2013JD021374

Martin, S. T., Artaxo, P., Machado, L., Manzi, A. O., Souza, R. A. F., & Schumacher, C. et al. (2017). The Green Ocean Amazon Experiment (GoAmazon2014/5) observes pollution affecting gases, aerosols, clouds, and rainfall over the rain forest. *Bulletin of the American Meteorological Society*, *98*, 981–997. https://doi.org/10.1175/BAMS-D-15-00221.1

Masunaga, H., & Luo, Z. J. (2016). Convective and large-scale mass flux profiles over tropical oceans determined from synergistic analysis of a suite of satellite observations. *Journal of Geophysical Research: Atmospheres*, *121*. https://doi.org/10.1002/2016JD024753

Mather, J. H., & Voyles, J. W. (2013). The ARM climate research facility: A review of structure and capabilities. *Bulletin of the American Meteorological Society*, *94*, 377–392.

May, P. T., & Rajopadhyaya, D. K. (1999). Wind profiler observations of vertical motion and precipitation microphysics of a tropical squall line. *Monthly Weather Review*, *124*(4), 621–633.

North, K. W., Oue, M., Kollias, P., Giangrande, S. E., Collis, S. M., & Potvin, C. K., (2017). Vertical air motion retrievals in deep convective clouds using the ARM scanning radar network in Oklahoma during MC3E. *Atmospheric Measurement Techniques*, *10*, 2785–2806. https://doi.org/10.5194/amt-10-2785-2017

Platnick, S., King, M. D., Ackerman, S. A., Menzel, W. P., Baum, B. A., Riedi, J. C., & Frey, R. A. (2003). The MODIS cloud products: Algorithms and examples from Terra. *IEEE Transactions on Geoscience and Remote Sensing*, *41*(2), 459–473.

Sanderson, B. M., Piani, C., Ingram, W. J., Stone, D. A., & Allen, M. R. (2008). Toward constraining climate sensitivity by linear analysis of feedback patterns in thousands of perturbed-physics GCM simulations. *Climate Dynamics*, *30*, 175–190. https://doi.org/10.1007/s00382-007-0280-7

Stephens, G. L., Vane, D. G., Boain, R. J., Mace, G. G., Sassen, K., & Wang, Z. et al. (2002). The CloudSat mission and the A-TRAIN: A new dimension to space-based observations of clouds and precipitation. *Bulletin of the American Meteorological Society*, *83*, 1771–1790.

Stephens, G. L., Vane, D. G., Tanelli, S., Im, E., Durden, S., & Rokey, M. (2008). CloudSat mission: Performance and early science after the first year of operation. *Journal of Geophysical Research*, *113*, D00A18. https://doi.org/10.1029/2008JD009982

Stephens, G. L., & Kummerow, C. D. (2008). The remote sensing of clouds and precipitation from space: A review. *Journal of the Atmospheric Sciences*, *64*, 3742–3765. https://doi.org/10.1175/2006JAS2375.1

Takahashi, H., & Luo, Z. (2012). Where is the level of neutral buoyancy for deep convection? *Geophysical Research Letters*, *39*, L15809. https://doi.org/10.1029/2012GL052638

Takahashi, H., Luo, Z. J., & Stephens, G. L. (2017). Level of neutral buoyancy, deep convective outflow, and convective core: New perspectives based on 5 years of CloudSat data. *Journal of Geophysical Research: Atmospheres*, *122*. https://doi.org/10.1002/2016JD025969

Tridon, F., Battaglia, A., Kollias, P., Luke, E., & Williams, C. R. (2013). Signal postprocessing and reflectivity calibration of the Atmospheric Radiation Measurement Program 915-MHz wind profilers. *Journal of Atmospheric and Oceanic Technology*, *30*, 1038–1054. https://doi.org/10.1175/JTECH-D-12-00146.1

Wang, D., Giangrande, S. E., Bartholomew, M. J., Hardin, J., Feng, Z., Thalman, R., & Machado, L. A. T. (2018). The Green Ocean: Precipitation insights from the GoAmazon2014/5 experiment. *Atmospheric Chemistry and Physics*, *18*, 9121–9145. https://doi.org/10.5194/acp-18-9121-2018

Wang, D., Giangrande, S. E., Feng, Z., Hardin, J. C., & Prein, A. F. (2020). Updraft and downdraft core size and intensity as Revealed by radar wind profilers: MCS observations and idealized model comparisons. *Journal of Geophysical Research: Atmospheres*, *125*, e2019JD031774. https://doi.org/10.1029/2019JD031774

Wang, D., Giangrande, S. E., Schiro, K., Jensen, M. P., & Houze, R. A. (2019). The characteristics of tropical and midlatitude mesoscale convective systems as revealed by radar wind profilers. *Journal of Geophysical Research: Atmosphere*, *124*, 4601–4619. https://doi.org/10.1029/2018JD030087

Wang, C., Luo, Z. J., Chen, X., Zeng, X., Tao, W.-K., & Huang, X. (2014). A physically based algorithm for non-blackbody correction of cloud-top temperature and application to convection study. *Journal of Applied Meteorology and Climatology*, *53*, 1844–1857.

Wang, C., Luo, Z. J., & Huang, X. (2011). Parallax correction in collocating CloudSat and Moderate Resolution Imaging Spectroradiometer (MODIS) observations: Method and application to convection study. *Journal of Geophysical Research*, *116*, D17201. https://doi.org/10.1029/2011JD016097

Williams, C. R. (2012). Vertical air motion retrieved from dual-frequency profiler observations. *Journal of Atmospheric and Oceanic Technology*, *29*, 1471–1480. https://doi.org/10.1175/JTECH-D-11-00176.1

Winker, D. M., Pelon, J., Coakley, J. A. Jr., Ackerman, S. A., Charlson, R. J., & Colarco, P. R. et al. (2010). The CALIPSO mission: A global 3D view of aerosols and clouds. *Bulletin of the American Meteorological Society*, *91*, 1211–1229. https://doi.org/10.1175/2010BAMS3009.1

Yuter, S. E., & Houze, R. A. (1995). Three-dimensional kinematic and microphysical evolution of Florida cumulonimbus, Part II: Frequency distributions of vertical velocity, reflectivity, and differential reflectivity. *Monthly Weather Review*, *123*, 1941–1963.

Zipser, E. J. (2003). Some views on "hot towers" after 50 years of tropical field programs and two years of TRMM data. *Meteorological Monographs*, *51*, 49–58.